Improved neutron capture cross section of ^{239}Pu

S. Mosby,[1,*] T. A. Bredeweg,[1] A. Chyzh,[1] A. Couture,[1] R. Henderson,[2] M. Jandel,[1] E. Kwan,[2,†] J. M. O'Donnell,[1] J. Ullmann,[1] and C. Y. Wu[2]

[1]*Los Alamos National Laboratory, Los Alamos, New Mexico 87545, USA*

[2]*Lawrence Livermore National Laboratory, Livermore, California 94550, USA*

(Received 8 November 2013; published 12 March 2014)

The ^{239}Pu(n,γ) cross section has been measured over the energy range 10 eV to 1 keV using the Detector for Advanced Neutron Capture Experiments (DANCE) at the Los Alamos Neutron Science Center as part of a campaign to produce precision (n,γ) measurements on ^{239}Pu. Fission coincidences were measured with a parallel-plate avalanche counter and used to measure the prompt fission γ-ray spectrum in this region to accurately characterize background. The resulting (n,γ) cross section is generally in agreement with current evaluations. The experimental method utilizes much more detailed information than past measurements on ^{239}Pu and can be used to extend the measurement to higher incident neutron energies.

DOI: 10.1103/PhysRevC.89.034610 PACS number(s): 25.40.Lw

I. INTRODUCTION

Accurate measurements of the ^{239}Pu(n,γ) reaction are needed by nuclear energy and defense programs. The Advanced Reactor Concepts (ARC) program is considering the next generation of reactor designs. The designs under consideration all have a faster neutron spectrum than traditional light water reactors, and require improved nuclear data in the keV region. In particular, sensitivity studies [1,2] identified the ^{239}Pu(n,γ) cross section above 2 keV as a need for the ARC program.

Fissile isotopes present unique challenges to measurement techniques which rely on γ-ray detection. In particular, fission is an open reaction channel which competes strongly with capture and so is an additional source of background in the data. Therefore, some method of characterizing the properties of fission in the system of interest and properly subtracting it to obtain an accurate residual capture spectrum must be used.

Past work on the ^{239}Pu(n,γ) cross section ended in the 1970's [3–6] (see Fig. 1), and the accuracy of the measurements was limited by the technology available at the time. Large cadmium-loaded liquid scintillator tanks were used to detect both capture and fission γ rays as well as fission neutrons, and in some cases fission events were tagged by a delayed scintillator pulse due to thermalized neutrons capturing on cadmium. This system does not allow for detailed knowledge of the various components of the observed γ-ray spectrum, which is useful for confirming a good understanding of all backgrounds. Furthermore, the facilities of the time could not compete with current neutron fluxes which resulted in less desirable signal to noise ratios than are obtainable today. Finally, electronics of the time mandated dead time corrections which introduce additional uncertainty in resonance strength–something which can be avoided with modern technology.

Figure 1 shows the prior measured cross sections as a function of energy, and the effect of these limitations can be seen coming into play. It is clear that Refs. [5,6] provide the most information; indeed, the ENDF/B-VII.1 [7] evaluation in this energy region is based on those datasets. The JENDL-4.0 [8] evaluation is nearly identical to ENDF and the two curves lie almost completely atop each other. It is worth mentioning that Ref. [6] reports an absorption cross section, so their reported fission cross section was subtracted off in order to compare with other measurements. It is clear that the valleys between resonances still contain significant background, and there are resonances at 18, 21, and 46 eV which are reported to result from tungsten contamination in the samples used for those measurements. While measurements [5,6] provide immensely useful information, it is clear that a new, more detailed measurement is desirable.

The Detector for Advanced Neutron Capture Experiments (DANCE) [9], in conjunction with the beams available at the Los Alamos Neutron Science Center (LANSCE), provides a novel method of obtaining these cross sections in light of the constraints for fissile isotopes [10]. A thin ^{239}Pu target mounted inside a charged particle detector is used to characterize the prompt fission γ spectrum and measure the capture cross section simultaneously. The resulting information could be used in conjunction with a more massive target to extend the measurement range to higher neutron energies.

II. EXPERIMENTAL SETUP

The DANCE setup is located at flight path 14 of the Lujan Neutron Scattering Center at LANSCE [11] which views the upper tier water moderator. Spallation neutrons are produced by a pulsed 800 MeV proton beam with a repetition rate of 20 Hz impinging on a pair of tungsten targets [12]. They are then reflected by the moderator and travel down a 20.2-m flight path to the target location. The tightly collimated beam views only the moderator, and direct γ rays from the tungsten targets are eliminated. The beam flux at the target position is approximately 3×10^5 n/s cm^2 energy decade.

DANCE itself consists of 160 BaF_2 crystals which cover a solid angle of approximately 3.5π with a single-γ-ray efficiency of 85%. A detailed description of the detector

*smosby@lanl.gov

†Current address: National Superconducting Cyclotron Laboratory, East Lansing, Michigan 48824, USA.

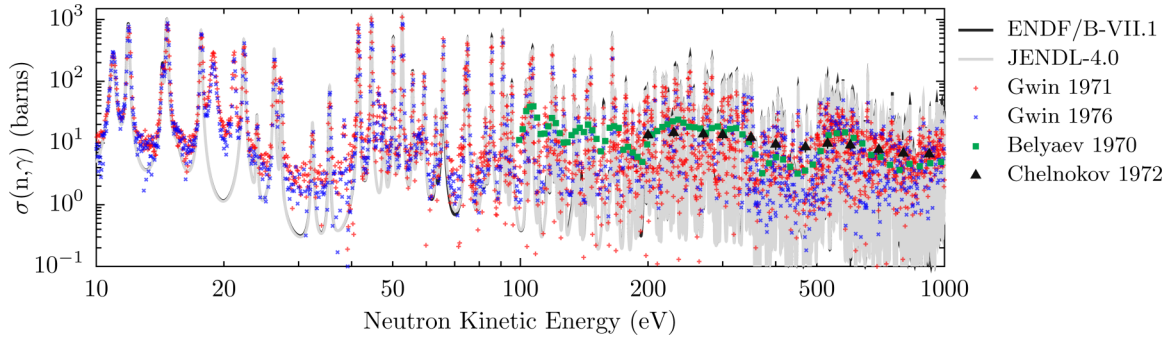

FIG. 1. (Color online) Prior measurements of ^{239}Pu(n,γ), with Gwin 1971, Gwin 1976, Belyaev 1970, and Chelnokov 1972 from Refs. [3–6] respectively.

and its response can be found in [13]. For this experiment, 937 μg of ^{239}Pu target material was electroplated onto both sides of a 3 μm Ti backing and covered by a pair of 1.4 μm Al Mylar windows for containment and protection of the sample. This assembly served as the central cathode for a parallel-plate avalanche counter (PPAC) which was arranged in an anode-cathode-anode configuration with the cathode at ground and the anodes operated at 375 V. The outer windows for the PPAC consisted of 25.4 μm of Kapton. The active area of the PPAC was 2.54 cm in diameter, and the entire assembly was placed at the target location in the center of DANCE. Isobutane gas at 4.5 torr with a flow rate of 4 cc/m filled the active volume of the PPAC. The target and PPAC were fabricated at LLNL, and the sample material enriched to 99.97% ^{239}Pu. The primary contaminant was ^{240}Pu, and the sample composition can be found in Table I. Details of the PPAC design and fabrication can be found in [14].

The details of the data acquisition and analysis systems are described in [15,16], with a summary provided below. Signals for both DANCE crystals and the PPAC were digitized in Acqiris DC265 digitizers, with 8-bit resolution (7.6 effective bits) and 2-ns sampling intervals. Each DANCE crystal signal was processed by two independent digitizer channels. In this experiment, the data were taken in the double continuous acquisition mode (referred to as mode 2 in [15]). This mode involves triggering the digitizers on the proton-beam time-reference signal (T0) and taking a 250-μs waveform. This waveform is processed online by a front-end computer, which locates peaks in the waveform and writes 32 points over the fast component of the signal as well as five charge integrals for each waveform to disk. The two digitizer sets can be set to have different acquisition windows relative to the T0, and within these windows there is no hardware dead time. Fast signals from the PPAC were processed in a similar way and used for coincidence timing between fission fragments and γ rays with a charged particle detection efficiency of roughly 65%.

TABLE I. Sample composition.

Nuclide	Fraction (%)
^{239}Pu	99.97
^{240}Pu	0.03

III. ANALYSIS

This work reports the use of a thin target in conjunction with a PPAC to make a cross section measurement from 10 eV to 1 keV. The analysis proceeded in three basic modes: background subtraction, cross section calculation, and systematic uncertainty estimation. For the purposes of this analysis, γ-ray spectra were characterized in terms of their total energy and multiplicity. Total energy ($E_{\rm sum}$) refers to the total γ-ray energy release of a physics event. Because all γ rays from any DANCE crystal inside a given 250-μs waveform are written to disk, the definition of what constitutes a "physics event" is adjustable in the analysis software. For this analysis, a physics event was defined as all detector signals arriving within a software defined coincidence window (10 ns for DANCE crystals and 15 ns for PPAC/DANCE coincidences).

There are two possible definitions of multiplicity within DANCE. The first is simply the crystal multiplicity $M_{\rm cr}$ which is defined as the number of crystals which fired during a given physics event. Due to detector response, particularly Compton-scatter effects between adjacent crystals, this definition is less useful than the alternative cluster multiplicity $M_{\rm cl}$. A clustering algorithm is used to locate sets of adjacent crystals which fired during a physics event and their energies are summed. The total number of resulting clusters is referred to as $M_{\rm cl}$. While this parameter still does not represent the true γ-ray multiplicity due to detector response, it is robust for eliminating background.

Energy and timing calibrations were performed run by run. Energy calibrations utilized intrinsic α radioactivity within the DANCE crystals. Selection of α-decay events involved gating on multiplicity-one events which passed a pulse-shape-discrimination gate. BaF_2 has fast and slow light components, and the fast component is greatly suppressed in α-decay events compared to γ rays. Timing calibrations were performed using Compton-scattered γ rays. A wide (50 ns) coincidence gate was used for event building, and the time difference between Compton events in neighboring crystals was used to calculate their relative timing properties. These relative times were chained together to tie the entire array to a common timing basis.

The background subtraction itself had three components: neutron-induced fission, scattered neutrons, and γ rays. The qualitative process is shown in terms of the $E_{\rm sum}$ spectrum

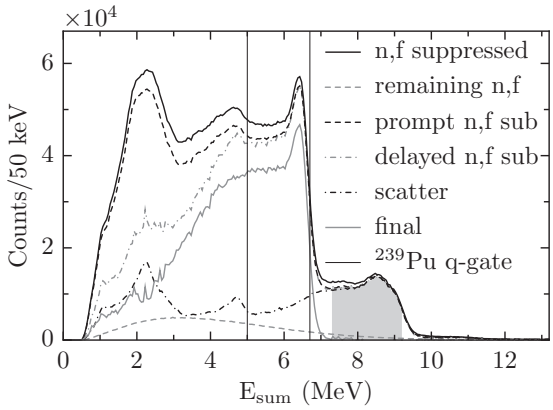

FIG. 2. Total γ-ray energy spectra for E_n from 37 eV to 1 keV and $3 \leqslant M_{\rm cl} \leqslant 5$ demonstrating the background subtraction process. See text for details.

for the energy range 37 eV to 1 keV in Fig. 2, but the exact procedure was performed bin-by-bin across the entire neutron energy spectrum since all backgrounds have some energy dependence. Most prompt fission is removed from the spectrum by gating on anti-coincidence data between DANCE and the PPAC, but the PPAC is not 100% efficient so the remaining fission must be accounted for. Therefore, the fission component of the spectrum is characterized from PPAC coincidence data (grey dashed line) and subtracted to form the intermediate dashed black line. Delayed fission is characterized by taking data prior to the beam T0 and normalizing by the time width of each neutron energy bin to produce the grey dot-dashed line.

The active PPAC was removed and a blank PPAC with no ^{239}Pu inserted to define a spectral shape for backgrounds resulting from scattered beam neutrons and γ rays from the moderator and collimation. This spectral shape was normalized to the data in the region 7.3–9.2 MeV (shaded region), where the spectrum is dominated by capture on barium in the DANCE crystals themselves. The resulting (black dot-dashed) line is then subtracted to produce the solid grey line. A cut is placed on the ^{239}Pu capture Q-value peak of 6.53 MeV (vertical lines) to identify those counts resulting from radiative capture.

A. Fission subtraction details

Prompt fission γ rays are emitted in coincidence with charged fission fragments, so an anti-coincidence gate between DANCE and the PPAC can be used to suppress this background. However, the PPAC efficiency is less than 1, so a residual prompt fission background remains. The prompt fission subtraction process involved a set of scaling factors and integrals calculated bin-by-bin in terms of neutron kinetic energy. The prompt fission contamination yield can be expressed as

$$Y_{\rm pfis} = (1 - \epsilon_{\rm ppac}) N_{\rm capcoinc}, \quad (1)$$

where $Y_{\rm pfis}$ is the number of fission background counts, $\epsilon_{\rm ppac}$ is the efficiency of the PPAC, and $N_{\rm capcoinc}$ is the number

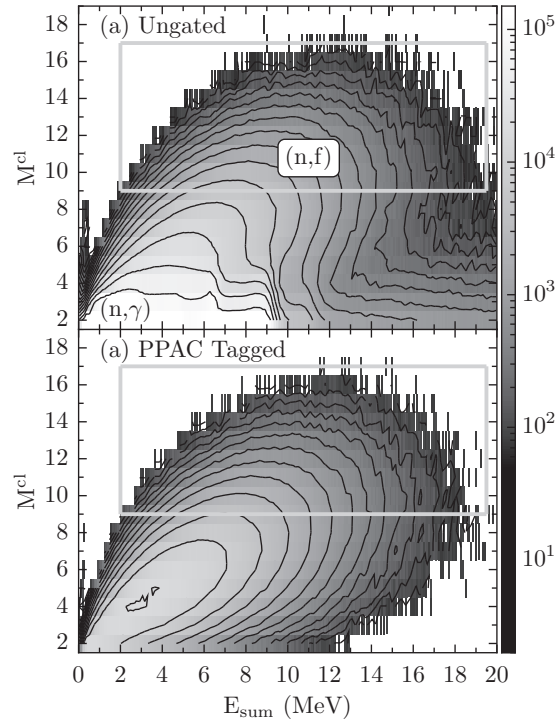

FIG. 3. $M_{\rm cl}$ vs $E_{\rm sum}$ for (a) ungated and (b) PPAC coincidence. The box defined a region where only fission contributes to the spectrum, and is used to determine the PPAC efficiency.

of events the PPAC observed within the capture gates of cluster multiplicity $M_{\rm cl}$ 3–5 and total γ-ray energy $E_{\rm sum}$ of 5–6.7 MeV. These multiplicity and energy gates were used for all further analysis of the capture yield. Figure 3 illustrates how the PPAC efficiency was calculated. Figure 3(a) shows two different structures: a broad distribution roughly along the diagonal which corresponds to fission [see Fig. 3(b)], and a low multiplicity "shelf" which corresponds to neutron capture and scattered background. The boxed high-energy, high-multiplicity region's only contributor is fission, so the ratio of all DANCE events to those in coincidence with the PPAC in that region defines the efficiency. This efficiency was calculated as a running 7-point average as a function of energy to account for minor fluctuations across resonances, and determined to be $65.0 \pm 1.4\%$.

The PPAC is sensitive to the α-decay background originating from the sample material. As shown in Fig. 4, this background appears at the lower edge of the signal-height spectrum, but has a tail that runs under and significantly contaminates the fission part of the spectrum. The background is partially eliminated by requiring the signal to be above the noted threshold of 300 units. When a coincidence with DANCE $M_{\rm cl} \geqslant 3$ is required, the α tail is largely eliminated (black solid curve) but the threshold is still used to reject low-signal events. The calculated efficiency as a function of threshold is shown as the dashed line.

The fission process produces many long-lived nuclear species which decay, and potentially produce γ rays, on timescales much longer than the coincidence window. Furthermore, these secondary decays do not produce signals

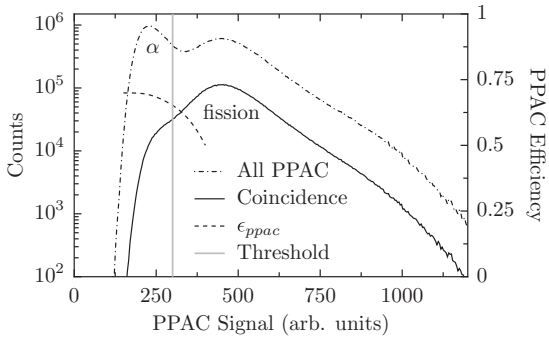

FIG. 4. PPAC pulse height spectrum for coincidence events with $M_{\rm cl} \geqslant 3$ (solid black) and ungated (dot-dashed black). The dashed curve shows PPAC efficiency as a function of threshold, and the vertical line denotes the threshold used in this analysis.

in the PPAC so there is no explicit detector tag which can suppress them. The buildup of long-lived fission fragments in the sample ultimately contributed significantly to the observed signal for $E_{\rm sum} \leqslant 4$ MeV. The decay time of this background was ∼40 min.

In order to characterize and subtract this source of background, we used our digitizers' look-back window to take data 10 μs prior to the beam T0 (see Fig. 5). This look-back window results from the circular buffering system in the digitizers such that data can be taken prior to the arrival of a trigger. Events in the time window of −10 to −0.9 μs were used to determine the background rate and spectral shape. Since this background data were taken in parallel with the production data, the resulting background $Y_{\rm dfis}$ can be expressed as

$$Y_{\rm dfis} = \frac{\Delta T_{\rm ebin}}{\Delta T_{\rm lb}} N_{\rm lb}, \tag{2}$$

where $N_{\rm lb}$ is the number of counts in the look-back window which satisfy the capture gate, and $\Delta T_{\rm ebin}$ and $\Delta T_{\rm lb}$ are the time widths of each neutron energy bin analyzed and the look-back window, respectively. The resulting effect on the observed γ-ray spectrum is shown in Fig. 2.

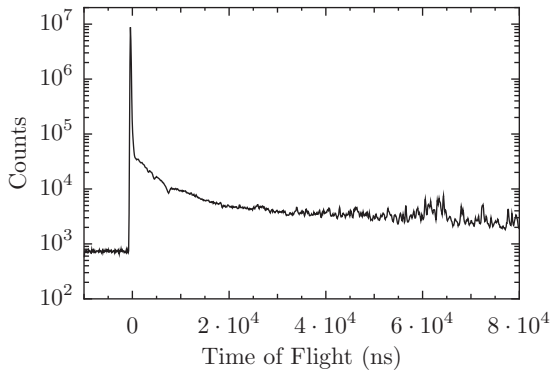

FIG. 5. Time of flight spectrum for $3 \leqslant M_{\rm cl} \leqslant 5$ demonstrating the look-back window and the first 80 μs of the acquisition window. Negative times correspond to events occurring prior to beam T0 and are used to characterize delayed fission background. The γ flash from the moderator is clearly visible.

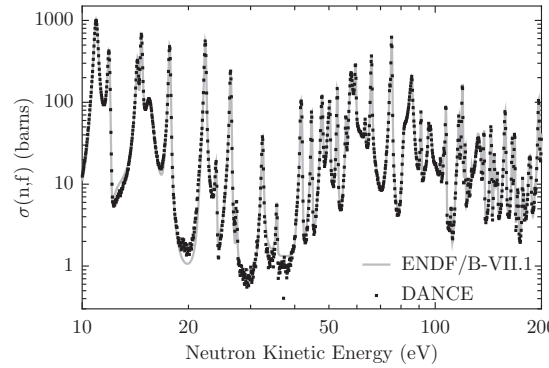

FIG. 6. DANCE fission cross section compared to evaluation.

B. Scattered neutron and γ-ray subtraction details

Another source of background results from neutrons scattering from the sample material and PPAC assembly, moderating in the large volume of BaF_2 and capturing on the detector material itself. Of particular interest are $^{135-138}$Ba, which have capture Q values of 9.108, 6.906, 8.612, and 4.723 MeV, respectively. Also, γ rays can be scattered in the moderator or produced in collimation upstream of DANCE and ultimately be detected in DANCE crystals. This source of background contributes most dominantly below 3 MeV in the $E_{\rm sum}$ spectrum. The combined effect of these scattered backgrounds was determined by normalizing a scattered background spectral shape to the production data. This proceeded by taking data with a blank PPAC placed at the target location. The contamination of the capture gate and the capture yield could then be expressed as

$$Y_{\rm cap} = N_{\rm nofis} - Y_{\rm pfis} - Y_{\rm dfis} - A_{\rm norm} N_{\rm scat}, \tag{3}$$

$$A_{\rm norm} = I_{\rm prod}/I_{\rm blank}, \tag{4}$$

where $N_{\rm nofis}$ is the anti-PPAC gated yield, $N_{\rm scat}$ is the number of scattered background inside the capture gate of $M_{\rm cl}$ 3–5 and $E_{\rm sum}$ 5–6.7 MeV, and $A_{\rm norm}$ is a scaling factor between the blank runs and production. $I_{\rm prod}$ is the integral number of counts lying between 7.3 and 9.2 MeV for the target-in data, and $I_{\rm blank}$ is the same for the blank PPAC runs (see Fig. 2, shaded region). The integration region is very cleanly populated by capture on $^{135-137}$Ba and lies well above the ^{239}Pu capture Q value. Again, this procedure was performed as a function of incident neutron energy to capture changes in the structure and strength of the background.

C. Cross section calculation

The Lujan Center's beam pulse structure, use of a moderator, and Doppler broadening effects mandate the use of a resolution function in any discussion of results or analysis. Therefore, the code SAMMY7 [17] was used to broaden ENDF/B-VII.1 cross sections for the system response using the Rensselaer Polytechnic Institute broadening expression with parameters determined by Koehler [18]. The capture cross section itself was measured as a ratio to fission. Because the experiment could observe simultaneous yields for both the fission and capture using the same target, this cross section

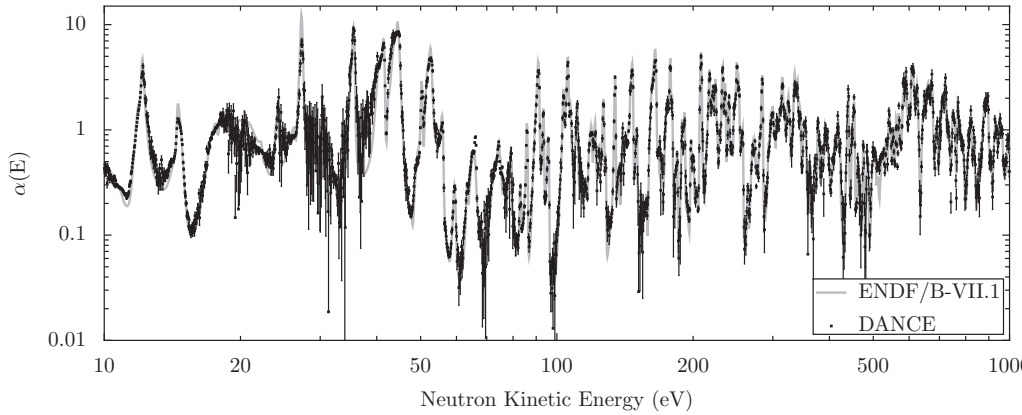

FIG. 7. DANCE capture-to-fission ratio α compared to evaluation.

can be expressed as

$$\sigma_{n\gamma}(E) = A_{n\gamma}\sigma_{nf}(E)\frac{Y_{\rm cap}(E)}{N_{\rm coinc}(E)}, \tag{5}$$

where $\sigma_{n\gamma}(E)$ is the capture cross section as a function of neutron energy, $A_{n\gamma}$ is a scaling factor relating the capture to fission yield ratio to a cross section ratio, $\sigma_{nf}(E)$ is the SAMMY-broadened ENDF/B-VII.1 fission cross section, and $N_{\rm coinc}$ is the number of coincidences of the PPAC with DANCE which satisfied a $M_{\rm cl} \geqslant 3$ gate. $A_{n\gamma}$ was calculated using the evaluated cross section for capture and fission from the 17–18 eV resonance, expressed as

$$A_{n\gamma} = \frac{\int \sigma_{nf}(E)dE}{\int \sigma_{n\gamma}(E)dE}\frac{\int N_{\rm coinc}dE}{\int Y_{\rm cap}dE}. \tag{6}$$

This method eliminates uncertainties in the neutron flux, detector efficiency, and sample size and illumination. It does, however, require a robust fission tag so that $N_{\rm coinc}$ would be reliable across the neutron energy range of interest. Therefore, the measured fission yield was used to calculate a fission cross section and compared to the SAMMY-broadened ENDF cross section. The result is shown in Fig. 6 where the evaluated and measured results are shown to be in excellent agreement. With a proven fission tag and detailed background subtractions performed, the capture-to-fission ratio and capture cross section can be measured with confidence. This intermediate capture-to-fission ratio α is shown in Fig. 7. In general α tracks very well, with some detailed features. In general, it seems that sharp changes in the ratio are somewhat broadened in the DANCE data compared to evaluation. SAMMY was used to vary the target thickness to explore possible multiple scatter and self-absorption effects. Scatter and absorption effects were seen to have negligible impact on the measured α across the simulated sample mass range of 0.1–100 mg. The simulated sample mass range was selected to simulate conditions much more extreme than the sample mass of 937 μg. Moreover, the effect is seen in the tens of eV neutron energy range where Doppler broadening dominates the broadening of data relative to evaluation. Therefore the resolution function itself is not a likely source for the broadening of sharp changes in α observed in DANCE compared to evaluation.

D. Uncertainty analysis and signal/noise

Statistical uncertainties for all yields and associated scaling factors and normalization constants were propagated through all previously mentioned calculations, while systematic uncertainties were estimated for the parameters $\epsilon_{\rm ppac}$, $A_{\rm norm}$, $A_{n\gamma}$, and σ_{nf}. These parameters and their associated values are noted in Table II. On resonance, systematic uncertainties dominate and are $\sim$3%.

The signal-to-noise ratio is a useful metric to understand how important the background measurements and subtractions are. This quantity can be calculated from

$$R_{\rm sn} = \frac{Y_{\rm cap}}{Y_{\rm pfis} + Y_{\rm dfis} + A_{\rm norm}N_{\rm scat}}. \tag{7}$$

The ratio was greater than unity for the most of the measured region, only dipping below 1 in the low cross section "valleys" between resonances. At resonance peaks, the ratio was consistently above 5. In the interest of precision measurements it is therefore important to have a well characterized background, but measurements of the strong resonances should be very robust.

IV. RESULTS AND DISCUSSION

The full measured cross section in the range 10 eV to 1 keV is shown in Fig. 8 compared to ENDF/B-VII.1 folded with the DANCE flight path resolution function. In general our measurement and the evaluation track fairly well, with a few isolated resonances being significantly different, e.g., those near 66 and 510 eV. It is interesting to note that in both cases our data are higher than the evaluation and in both cases the fission

TABLE II. Systematic uncertainties.

Parameter	Description	$\Delta X/X$%
$\epsilon_{\rm ppac}$	PPAC efficiency	1.4
$A_{\rm norm}$	Scattered background scaling	1.5
$A_{n\gamma}$	(n,γ) Cross section normalization	2
σ_{nf}	Reference (n,f) cross section	1

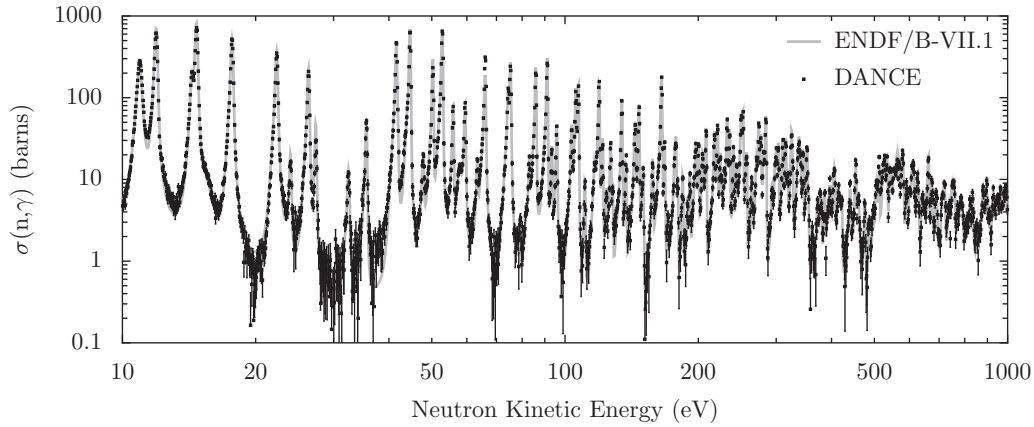

FIG. 8. DANCE α-derived ^{239}Pu(n,γ) cross section compared to ENDF/B-VII.1.

cross section is significantly higher than the capture cross section. Details of the 60–90 eV region of the spectrum are shown in Fig. 9, where it is clear that the 66-eV resonance is not well described by the evaluation but nearby resonances are. Table III compares the integral cross sections for several regions and again our measurement tracks fairly closely with evaluations: 8 of the 10 of the regions are within 4% of the evaluation, and the sum over the entire 10–1000 eV region is within 1%.

Comparing to the prior work in Fig. 1, it is clear that our background subtraction is more advanced. For example, in the weak capture region between 30 and 40 eV, our cross section drops in line with evaluations and runs almost an order of magnitude lower than the datasets [5,6]. Furthermore, the datasets report a trio of resonances at 18, 21, and 46 eV which are stated to be tungsten contamination in the sample. This work used a very pure sample and these contaminant resonances were not observed in the data. The datasets from Refs. [3,4] do not have the granularity to see resonance structures at all and are not used in the ENDF evaluation.

Future work will focus on extending the measurement to higher incident neutron energies, where the signal-to-noise ratio degrades rapidly due to decreasing neutron flux and rising backgrounds (see Fig. 5 where the count rate rises rapidly at low time of flight despite the neutron flux falling off). Increased target mass will directly improve signal to noise, but a significant improvement precludes the use of a PPAC. The α-decay counting rate will be too high, and the fission fragment detection efficiency will suffer due to the large mass. Fortunately, as shown in Fig. 3 we have already characterized the prompt fission spectrum using DANCE, and the $M_{\rm cl} \geqslant 8$ portion of the spectrum is completely dominated by fission. Therefore, we can use the fission spectrum from this experiment and normalize to any future data to properly subtract the fission background component. Such a procedure has already been performed successfully on ^{235}U [10].

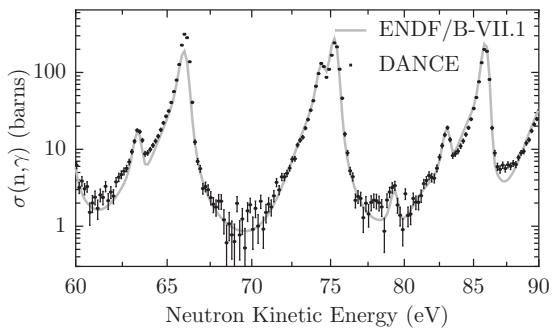

FIG. 9. DANCE ^{239}Pu(n,γ) cross section compared to ENDV/B-VII.1 in the 60–90 eV region.

V. SUMMARY

In this work, the ^{239}Pu capture-to-fission ratio α has been measured and the ^{239}Pu(n,γ) cross section deduced for the neutron energy region 10 eV to 1 keV. This measurement largely confirms the current evaluation, but differences in the individual resonance strengths are observed in several cases. The present work represents a significant advancement in experimental technique over prior work, and the detailed background suppression and subtraction methods can be observed to result in a marked improvement for weak signal to noise regions. The signature of fission events in DANCE has been explored via coincidence measurements with a PPAC, which allows for possible future work to extend the measurement to higher neutron energies.

TABLE III. Integral cross sections (barns) for DANCE data and evaluation with deviations shown in percent.

Neutron energy (eV)	DANCE	ENDF/B-VII.1
10–100	3226 ± 107	3247 (−1)
100–200	1491 ± 49	1554 (−4)
200–300	1544 ± 51	1581 (−2)
300–400	926 ± 31	967 (−4)
400–500	425 ± 15	395 (7)
500–600	1091 ± 37	1084 (1)
600–700	665 ± 23	652 (2)
700–800	478 ± 17	494 (−3)
800–900	392 ± 15	364 (8)
900–1000	518 ± 19	505 (3)

ACKNOWLEDGMENTS

This work benefited from the use of the LANSCE accelerator facility. Work was performed under the auspices of the US Department of Energy by Los Alamos National Security, LLC, under Contract DE-AC52-06NA25396, and by Lawrence Livermore National Security, LLC, under Contract DE-AC52- 07NA27344.

[1] G. Aliberti, G. Palmiotti, M. Salvatores, T. K. Kim, T. A. Taiwo, M. Anitescu, I. Kodeli, E. Sartori, J. C. Bosq, and J. Tommasi, Ann. Nucl. Energy **33**, 700 (2006).

[2] M. Salvatores, G. Albierti, M. Dunn, A. Hogenbirk, A. Ignatyuk, M. Ishikawa, I. Kodeli, A. J. Koning, R. McKnight, R. W. Mills, P. Oblozinsky, G. Palmiotti, A. plompen, G. Rimpault, Y. Rugama, P. Talou, and W. S. Yang, Tech. Rep. Nuclear Energy Agency Organization for Economic Co-Operation and Development, 2008 (unpublished).

[3] F. N. Belyaev, K. G. Ignat'ev, S. I. Sukhoruchkin, S. P. Borovlev, V. V. Pavlov, M. B. Polozov, and A. N. Soldatov, in Proceedings of the Nuclear Data for Reactors Conference, Helsinki, 1970, p. 339 (unpublished).

[4] V. B. Chelnokov, V. A. Tolstikov, Ju. Ja. Stavisskij, A. A. Bergman, and A. E. Samsonov, Tech. Rep., Yaderno-Fizicheskie Issledovaniya, 1972 (unpublished).

[5] R. Gwin, L. W. Weston, G. Saussure, R. W. Ingle, J. H. Todd, F. E. Gillespie, R. W. Hockenbury, and R. C. Block, Nucl. Sci. Eng. **45**(1), 25 (1971).

[6] R. Gwin, E. G. Silver, R. W. Ingle, and H. Weaver, Nucl. Sci. Eng. **59**(2), 79 (1976).

[7] M. Chadwick *et al.*, Nucl. Data Sheets **112**, 2887 (2011).

[8] K. Shibata *et al.*, J. Nucl. Sci. Technol. **48**, 1 (2011).

[9] M. Heil, R. Reifarth, M. Fowler, R. Haight, F. Kaeppeler, R. Rundberg, E. Seabury, J. Ullmann, J. Wilhelmy, and K. Wisshak, Nucl. Instrum. Methods Phys. Res., Sect. A **459**, 229 (2001).

[10] M. Jandel *et al.*, Phys. Rev. Lett. **109**, 202506 (2012).

[11] P. W. Lisowski, C. D. Bowman, G. J. Russell, and S. A. Wender, Nucl. Sci. Eng. **106**(2), 208 (1990).

[12] M. Mocko and G. Muhrer, Nucl. Instrum. Methods Phys. Res., Sect. A **704**, 27 (2013).

[13] M. Jandel *et al.*, Nucl. Instrum. Methods Phys. Res., Sect. B **261**, 1117 (2007).

[14] C. Wu, A. Chyzh, E. Kwan, R. Henderson, J. Gostic, D. Carter, T. Bredeweg, A. Couture, M. Jandel, and J. Ullmann, Nucl. Instrum. Methods Phys. A **694**, 78 (2012).

[15] J. Wouters, A. Vicente, T. Bredeweg, E. Esch, R. Haight, R. Hatarik, J. O'Donnell, R. Reifarth, R. Rundberg, J. Schwantes, J. Ullmann, D. Vieira, and J. Wilhelmy, IEEE Trans. Nucl. Sci. **53**, 880 (2006).

[16] M. Jandel *et al.*, Phys. Rev. C **78**, 034609 (2008),

[17] N. M. Larson, Tech. Rep. ORNL/TM-9179/R7, 2006 (unpublished).

[18] P. E. Koehler (private communication).